

# $^{63}\text{Cu}$ and $^{35}\text{Cl}$ NMR Investigation of the $S = \frac{1}{2}$ Kagomé Lattice System $\text{ZnCu}_3(\text{OH})_6\text{Cl}_2$

T. Imai<sup>1</sup>, E. A. Nytko<sup>2</sup>, B.M. Bartlett<sup>2</sup>, M.P. Shores<sup>2</sup>, and D. G. Nocera<sup>2</sup>

<sup>1</sup>Department of Physics and Astronomy, McMaster University, Hamilton, ON L8S4M1, Canada

<sup>2</sup>Department of Chemistry, M.I.T., Cambridge, Massachusetts 02139

(Dated: February 8, 2020)

The possible realization of a spin-liquid state in  $\text{ZnCu}_3(\text{OH})_6\text{Cl}_2$  (herbertsmithite) has attracted much recent attention. We report a  $^{63}\text{Cu}$  and  $^{35}\text{Cl}$  NMR investigation of the Kagomé lattice formed by  $\text{Cu}^{2+}$  ions ( $S = \frac{1}{2}$ ). From the measurements of  $^{35}\text{Cl}$  NMR Knight shifts, we demonstrate that the local spin susceptibility develops a large distribution below  $\sim 125$  K. Low frequency spin fluctuations grow toward  $T = 0$  without the signature of a critical slowing down.

PACS numbers: 75.40.Gb, 76.60.-k

One of the major challenges in contemporary condensed matter physics is identifying a model material for investigating a *spin liquid* [1]. Searching for exotic electronic states without magnetic long range order constitutes a common thread in a wide range of research fields, from high temperature superconductivity to low dimensional quantum magnetism. A recent breakthrough in the hunt for a spin liquid state[2] is the successful synthesis [3] and characterization [4] of the Kagomé lattice  $\text{ZnCu}_3(\text{OH})_6\text{Cl}_2$ . As shown in Fig. 1, three  $\text{Cu}^{2+}$  ions form a triangle, and a network of corner-shared triangles form a Kagomé lattice. The  $S = \frac{1}{2}$  spin on Cu sites are mutually frustrated by antiferromagnetic super-exchange interaction  $J \sim 170$  K [4, 5], hence the possibility of a spin liquid ground state.

Over the last decade, many candidate materials were investigated as possible model system of a Kagomé lattice [6, 7, 8]. However, they mostly exhibit a magnetically ordered or spin-glass-like state at low temperatures. The new Kagomé material  $\text{ZnCu}_3(\text{OH})_6\text{Cl}_2$  distinguishes itself from earlier candidates, because the Cu sites have  $S = \frac{1}{2}$  and there is no evidence for magnetic long range order or freezing. Earlier bulk magnetic susceptibility  $\chi_{bulk}$ [4], specific heat[4], neutron scattering on powders[4], and  $\mu\text{SR}$ [9, 10] data established that  $\text{ZnCu}_3(\text{OH})_6\text{Cl}_2$  remains paramagnetic down to 50 mK. These findings point towards the possible existence of a frustrated spin liquid state. However, many physical properties of  $\text{ZnCu}_3(\text{OH})_6\text{Cl}_2$  call for a more thorough understanding. For example,  $\chi_{bulk}$  reveals a mysterious sharp *increase* below  $\sim 125$  K [4]. This differs from the predictions of various theoretical calculations: series expansions predict a *decrease* of  $\chi_{bulk}$  below  $T \sim J/6$  with a gap[11, 12], while the recent Dirac Fermion model predicts a linear behavior in  $T$  toward  $T = 0$  [13]. Furthermore, besides the observed absence of a spin gap [4], the Cu spin dynamics are not well understood.

In this *Letter*, we report a  $^{63}\text{Cu}$  and  $^{35}\text{Cl}$  NMR investigation of  $\text{ZnCu}_3(\text{OH})_6\text{Cl}_2$ . NMR is an ideal microscopic probe to investigate new materials, with a proven track record in quantum magnetism (see [14, 15, 16, 17] and references therein). Taking full advantage of the local nature of NMR, we uncover hitherto unknown properties of  $\text{ZnCu}_3(\text{OH})_6\text{Cl}_2$ . We demonstrate that the  $^{35}\text{Cl}$  nuclear

spin-lattice relaxation rate  $^{35}(1/T_1)$  shows an anomaly below 125 K with a peak at  $\sim 50$  K, and  $^{35}\text{Cl}$  NMR Knight shift develops a large distribution in the same temperature range. These findings imply that the local spin susceptibility  $\chi_{local}$  develops a site-by-site variation with decreasing temperature  $T$ , and the magnetic susceptibility  $\chi_{bulk}$  as observed by SQUID magnetometer simply represents a bulk average. We also demonstrate from the measurements of the  $^{63}\text{Cu}$  nuclear spin-lattice relaxation rate divided by temperature  $T$ ,  $^{63}(1/T_1 T)$ , that low frequency Cu spin fluctuations *grow* below  $\sim 30$  K. However, a Curie-Weiss fit down to 1.9 K leads to a small but negative Weiss temperature  $\theta = -1.2 \pm 1$  K. This is in marked contrast with the critical dynamics observed for typical two-dimensional or three-dimensional quantum Heisenberg model systems with power law or exponential divergence of  $1/T_1$  [14, 15, 16, 17].

In Fig. 2, we show representative  $^{35}\text{Cl}$  NMR lineshapes. For these measurements, we cured ceramics in a glue in a magnetic field of 9 Tesla. From powder x-ray diffraction measurements, we confirmed that some fraction of the ceramic powder is uniaxially aligned along the c-axis. In fact, we observe a sharp central peak near 35.02 MHz (marked as  $B//c$  in Fig. 2) arising from ceramic particles oriented along the c-axis, in addition to the typical quadrupolar split “double horns” observed in an earlier work[9] (marked as #1 and #2 in Fig. 2). Above 50 K, we could easily measure the c-axis peak frequency with FFT methods with extremely high precision, hence the corresponding Knight shift  $^{35}K_{peak}$  has very high precision. However, the  $^{35}\text{Cl}$  nuclear spin-lattice relaxation rate  $^{35}(1/T_1)$  has a peak at 50 K (see Fig. 4), and the whole  $^{35}\text{Cl}$  NMR lineshape begins to tail-off toward lower frequencies. Accordingly, we determined the high frequency edge of the c-axis peak as well as the half intensity position on the lower frequency side by point-by-point frequency scans. In what follows, we will call the Knight shifts corresponding to the edge and the half intensity position as  $^{35}K_{edge}$  and  $^{35}K_{1/2}$ , respectively.

We summarize the results of  $^{35}K$  in Fig. 3, together with the bulk average of the magnetic susceptibility,  $\chi_{bulk}$ , as observed by SQUID. Quite generally, we can

represent  $^{35}K$  as

$$^{35}K = A_{hf}\chi_{local} + ^{35}K_{chem}, \quad (1)$$

where  $A_{hf}$  is the magnetic hyperfine interaction between  $^{35}\text{Cl}$  nuclear spin and nearby Cu electron spins, and  $^{35}K_{chem}$  is a very small, temperature independent chemical shifts. In the present case, from the comparison with  $\chi_{bulk}$ , we estimate  $A_{hf} \sim -3.7 \pm 0.7 \text{ KOe}/\mu_B$ . The negative sign of  $A_{hf}$  makes the overall sign of  $^{35}K$  negative. Accordingly, we inverted the vertical scale of Fig. 3.

We wish to comment on two important aspects of Fig. 3. First,  $^{35}K_{peak}$  and  $^{35}K_{edge}$  follow Curie-Weiss behavior all the way from 295 K down to  $\sim 25$  K. This clearly differs from  $\chi_{bulk}$  which begins to deviate from Curie-Weiss behavior below  $\sim 125$  K [4]. On the other hand, series-expansion calculations indicate that the Kagomé lattice follows Curie-Weiss behavior down to  $T \sim J/6 \sim 25$  K [5, 11]. Our Knight shift data demonstrate that  $\chi_{local}$  of some segments of  $\text{Cu}^{2+}$  Kagomé lattice indeed show such behavior. Theoretical models also predict that below  $T \sim J/6 \sim 25$  K,  $\chi_{bulk}$  begins to decrease exponentially with a small gap[5, 11], or linearly[13]. As shown in Fig. 2, the  $^{35}\text{Cl}$  NMR lineshape begins to transfer some spectral weight to higher frequencies below 25 K. Recalling that  $A_{hf}$  is negative, this is consistent with vanishing spin susceptibility  $\chi_{local}$  near  $T = 0$  for some parts of the Kagomé lattice. Unfortunately, the very broad lineshape makes it difficult to draw a definitive conclusion on the low temperature behavior of  $^{35}K_{edge}$  below 25 K. Our results don't rule out the possibility that a small amount of defects or disorder in the Kagomé lattice may be causing the inhomogeneous line broadening below 25 K to *both* lower and higher frequencies (hence yielding an apparently smaller  $^{35}K_{edge}$ ).

A second important aspect of Fig. 3 is that the  $^{35}\text{Cl}$  NMR line gradually broadens to lower frequencies, hence  $^{35}K_{1/2}$  begins to deviate from the aforementioned Curie-Weiss fit in a manner similar to  $\chi_{bulk}$ . It is important to realize that  $^{35}(1/T_1)$  also begins to increase at  $\sim 125$  K (see Fig. 4). Below 50 K, where  $^{35}(1/T_1)$  shows a peak, the  $^{35}\text{Cl}$  NMR line shows a dramatic broadening to lower frequencies. Accidental superposition of the c-axis peak with the undesirable quadrupole peak #1 prevented us from determining  $^{35}K_{1/2}$  accurately between  $\sim 60$  K to 20 K. Yet it is clear from Fig. 2 and Fig. 3 that  $^{35}K_{1/2}$  follows the same trend as  $\chi_{bulk}$ . These results undoubtedly establish that *some segments of the Kagomé lattice have large and distributed local spin susceptibility  $\chi_{local}$* , and their temperature dependence is different from the smaller  $\chi_{local}$  as represented by  $^{35}K_{peak}$  and  $^{35}K_{edge}$ . The SQUID susceptibility data simply represent a bulk average of  $\chi_{local}$ .

In passing, we recall that earlier  $\mu\text{SR}$  Knight shift  $K_{\mu\text{SR}}$  measurements by Ofer *et al.* [9] showed an identical behavior between  $K_{\mu\text{SR}}$  and  $\chi_{bulk}$ . They concluded that the upturn of  $\chi_{bulk}$  below 50 K is not caused by impurity spins but is a bulk phenomenon. Our new results in Fig. 3 do not contradict these  $\mu\text{SR}$  data. It is

important to note that  $K_{\mu\text{SR}}$  was deduced by assuming a Gaussian distribution of  $\chi_{local}$ , hence by default  $K_{\mu\text{SR}}$  represents the central value of the presumed Gaussian distribution. That explains why  $K_{\mu\text{SR}}$  shows behavior similar to  $\chi_{bulk}$  and  $^{35}K_{1/2}$ .

Next, we turn our attention to the spin dynamics. Fig. 4 shows the temperature dependence of  $^{35}\text{Cl}$  nuclear spin-lattice relaxation rate  $^{35}(1/T_1)$  measured at the frequency corresponding to  $^{35}K_{peak}$  and  $^{35}K_{edge}$ . Quite generally, the nuclear spin-lattice relaxation, governed by low frequency spin fluctuations, may be expressed as[18],

$$\frac{1}{T_1} = T \frac{k_B \gamma_n^2}{\mu_B^2 \hbar} \sum_{\mathbf{q}} |F(\mathbf{q})|^2 \frac{\chi''(\mathbf{q}, \omega_n)}{\omega_n}, \quad (2)$$

where  $F(\mathbf{q})$  is the form factor of the hyperfine interactions between electron and nuclear spins.  $1/T_1$  measures the wave-vector  $\mathbf{q}$  integral of the imaginary part of the dynamical spin susceptibility  $\chi''(\mathbf{q}, \omega_n)$  at the NMR frequency  $\omega_n$ . Above  $\sim 125$  K, where  $\chi_{bulk}$  fits a Curie-Weiss law[4],  $^{35}(1/T_1) \sim 6 \text{ sec}^{-1}$  is temperature independent. Theoretically, we should expect  $^{35}(1/T_1)_{exc} \sim A_{hf}^2/J = constant$  in the exchange narrowing regime at  $T \gg J \sim 170$  K [19]. If we assume  $J \sim 170$  K and  $A_{hf} \sim -4 \text{ KOe}/\mu_B$ , the ballpark figure is  $^{35}(1/T_1)_{exc} \sim 4 \text{ sec}^{-1}$ .

Below  $T < J$ , if  $^{35}(1/T_1)$  senses only magnetic fluctuations,  $^{35}(1/T_1)$  should decrease as a short range order of Cu spins grow on the Kagomé lattice [19]. Instead, we found that  $^{35}(1/T_1)$  begins to increase below  $\sim 125$  K. This is precisely the temperature where  $\chi_{bulk}$  and  $^{35}K_{1/2}$  begin to deviate from a high temperature Curie-Weiss behavior. At 50 K, we find a robust peak for  $^{35}(1/T_1)$ . Absence of anomalies in the  $\mu\text{SR}$  data near 50 K [9] rules out a possibility that spin fluctuations slow down toward 50 K. We therefore conclude that *there is a mild slowing down of lattice fluctuations below 125 K. The fluctuation time scale slows down to our NMR frequency  $\sim 35$  MHz around 50 K, and enhance  $^{35}(1/T_1)$  through fluctuations of the electric field gradient (EFG)*. Since we do not find any noticeable changes in the  $I_z = \pm 3/2$  to  $\pm 1/2$  satellite lineshapes of  $^{35}\text{Cl}$  NMR, the change of the EFG at the  $^{35}\text{Cl}$  sites must be very small. The exact origin of the lattice fluctuations is still an open question at this time. One obvious possibility is a mild disorder arising from re-orientation of the OH bonding. This might possibly affect the Dzyloshinski-Moriya terms in spin Hamiltonian for this Kagomé lattice system and might naturally account for the upturn of  $\chi_{local}$  in this temperature regime[5].

In order to probe the intrinsic behavior of the Cu spin fluctuations, we searched for the resonance signals of  $^{63,65}\text{Cu}$ . Despite the initial pessimism arising from our expectation that the  $^{63,65}\text{Cu}$  NMR relaxation rates may be too fast to detect the signals, we were pleasantly surprised to be able to detect  $^{63,65}\text{Cu}$  NMR and NQR lines from 1.9 K up to  $\sim 40$  K, as shown in Fig. 5. The observed  $^{63}\text{Cu}$  NQR frequency  $^{63}\nu_Q = 40.6$  MHz is comparable to  $\sim 27$  MHz observed for  $\text{Cu}^{2+}$  ions in

a similar ligand environment in a square-lattice system in  $\text{Sr}_2\text{CuO}_2\text{Cl}_2$ [16]. However, the  $^{63}\text{Cu}$  NQR linewidth of 4 MHz observed in Fig. 5 is two orders of magnitude broader than in  $\text{Sr}_2\text{CuO}_2\text{Cl}_2$ , and implies that the EFG tensor at Cu sites has a nearly 10% distribution. The broad lineshape doesn't change at least up to  $\sim 40$  K. Possible sources of the large distribution of EFG include orientational disorder of the OH bonding and/or a small amount of alloying of Cu and Zn sites. We tried to see if the  $^{63}\text{Cu}$  NQR lineshape narrows above 50 K, but we were unable to detect the signal. Fig. 4 suggests that  $^{63}(1/T_1)$  must be faster than  $10^4$  sec $^{-1}$  above 50 K. According to our earlier experience[15, 16, 17],  $^{63}\text{Cu}$  NQR and NMR are not observable when the relaxation time is so fast. Our attempts to measure  $^{63,65}\text{Cu}$  NMR Knight shifts were also unsuccessful because the c-axis is not a high symmetry orientation for the EFG at Cu sites, hence the large and distributed EFG and Knight shift tensors smear the  $^{63,65}\text{Cu}$  NMR lineshapes even for aligned ceramics.

In Fig. 4, we compare the temperature dependence of the  $^{63}\text{Cu}$  nuclear spin-lattice relaxation rate  $^{63}(1/T_1)$  with  $^{35}(1/T_1)$ . We measured  $^{63}(1/T_1)$  by NMR techniques at the sharp edge observed in the high-field powder NMR lineshape, as marked by an arrow in Fig. 5. This edge corresponds to the Cu resonance when the direction of the external magnetic field is roughly orthogonal to the Cu-Cl bonding direction. Below  $\sim 30$  K,  $^{35}(1/T_1)$  asymptotes to  $^{63}(1/T_1)$ , and both show nearly identical behavior. A key qualitative feature to notice below 30 K is that  $^{63,35}(1/T_1)$  decreases roughly linearly with a *negative* curvature. This behavior is quite different from  $^{63}(1/T_1)$  observed for quantum spin systems with other geometries [17]. Without any sophisticated analysis, we immediately conclude that *paramagnetic spin fluctuations show no hint of the presence of magnetic in-*

*stabilities down to 1.9 K*. If the Kagomé lattice was critically slowing down toward a magnetic instability near  $T = 0$ ,  $^{63,35}(1/T_1)$  would increase toward  $T = 0$ , or at least change the sign of curvature to *positive*. We also show  $^{63,35}(1/T_1T)$  in the inset to Fig. 3. The growing  $^{63,35}(1/T_1T)$  toward  $T = 0$  means that *low-frequency Cu spin fluctuations grow with decreasing temperature* even though the Kagomé lattice remains paramagnetic. We could fit the data to a Curie-Weiss term with a constant background,  $^{63}(1/T_1T) = 95 + 1002/(T - \theta)$  with  $\theta = -1.2 \pm 1.0$  K. The negative sign of  $\theta$  reflects the negative curvature of  $^{63,35}(1/T_1)$  below  $\sim 30$  K, and signals that the growing spin fluctuations are *not* a manifestation of the tendency toward a magnetically ordered ground state. We also note that, if we fit the data to a power law  $^{63,35}(1/T_1) \sim T^\alpha$  as predicted by the recent Dirac Fermion model [13], we obtain a good fit with  $\alpha = 0.5 \pm 0.1$ . It remains to be seen whether the Dirac Fermion theories can predict this specific value of  $\alpha$ .

To conclude, we presented a site-by-site, local picture of the new Kagomé material  $\text{ZnCu}_3(\text{OH})_6\text{Cl}_2$  using NMR techniques. Our results establish that low-frequency spin fluctuations grow toward  $T = 0$  without a magnetic instability. This, as well as the  $^{35}\text{Cl}$  Knight shift data  $^{35}K_{\text{peak}}$  and  $^{35}K_{\text{edge}}$ , indicates that  $\text{ZnCu}_3(\text{OH})_6\text{Cl}_2$  may be indeed the best realization of the spin  $S = \frac{1}{2}$  Kagomé lattice Heisenberg model known to date. On the other hand, the peak of  $^{35}(1/T_1)$  and the large distribution of NMR Knight shift below 50K also indicate that there exist subtle perturbations to the ideal Heisenberg Kagomé lattice.

We thank Y.S. Lee, P.A. Lee, and S. De'Soto for helpful communications. The work at McMaster was supported by NSERC, CIAR, and CFI. We thank NSF for providing EAN and BMB with predoctoral fellowships, and DuPont for providing BMB with a Graduate Fellowship Award.

---

[1] P. W. Anderson, *Science* **253**, 1196 (1987).  
[2] *Physics Today*, **Feb. 2007**, 16 (2007).  
[3] M. P. Shores, E. A. Nytko, B. M. Bartlett, and D. G. Nocera, *J. Am. Chem. Soc.* **127**, 13462 (2005).  
[4] J. S. Helton, K. Matan, M. P. Shores, E. A. Nytko, B. M. Bartlett, Y. Yoshida, A. Suslov, Y. Qiu, J. H. Chung, D. G. Nocera, et al., cond-matt/0610539.  
[5] M. Rigol and R. R. P. Singh, cond-matt/0701087.  
[6] A. Keren, Y. J. Uemura, G. Luke, P. Mendels, M. Mekata, and T. Asano, *Phys. Rev. Lett.* **84**, 3450 (2000).  
[7] A. Fukaya, Y. Fudamoto, I. M. Gat, T. Ito, M. I. Larkin, A. T. Savici, and Y. J. Uemura, *Phys. Rev. Lett.* **91**, 207603 (2003).  
[8] F. Bert, D. Bono, P. Mendels, F. Ladieu, F. Duc, J. C. Trombe, and P. Millet, *Phys. Rev. Lett.* **95**, 087203 (2005).  
[9] O. Ofer, A. Keren, E. A. Nytko, and M. P. Shores, cond-matt/0610540.  
[10] P. Mendels, F. Bert, M. deVries, A. Olariu, A. Harrison, F. Duc, J. Trombe, J. Lord, A. Amato, and C. Baines, cond-matt/0610565.  
[11] N. Elstner and A. P. Young, *Phys. Rev. B* **50**, 6871 (2000).  
[12] F. Mila, *Phys. Rev. Lett.* **81**, 2356 (1998).  
[13] Y. Ran, M. Hermele, P. A. Lee, and X. G. Wen, cond-matt/0611414.  
[14] F. Borsa, M. Corti, T. Goto, A. Rigamonti, D. C. Johnston, and F. C. Chou, *Phys. Rev. B* **45**, 5756 (1992).  
[15] T. Imai, C. P. Slichter, K. Yoshimura, and K. Kosuge, *Phys. Rev. Lett.* **70**, 1002 (1993).  
[16] K. R. Thurber, A. W. Hunt, T. Imai, F. C. Chou, and Y. S. Lee, *Phys. Rev. Lett.* **79**, 171 (1997).  
[17] K. R. Thurber, T. Imai, T. Saitoh, M. Azuma, M. Takano, and F. C. Chou, *Phys. Rev. Lett.* **84**, 558 (2000).  
[18] T. Moriya, *J. Phys. Soc. Jpn.* **18**, 516 (1963).  
[19] T. Moriya, *Prog. Theor. Phys.* **16**, 23 (1956).

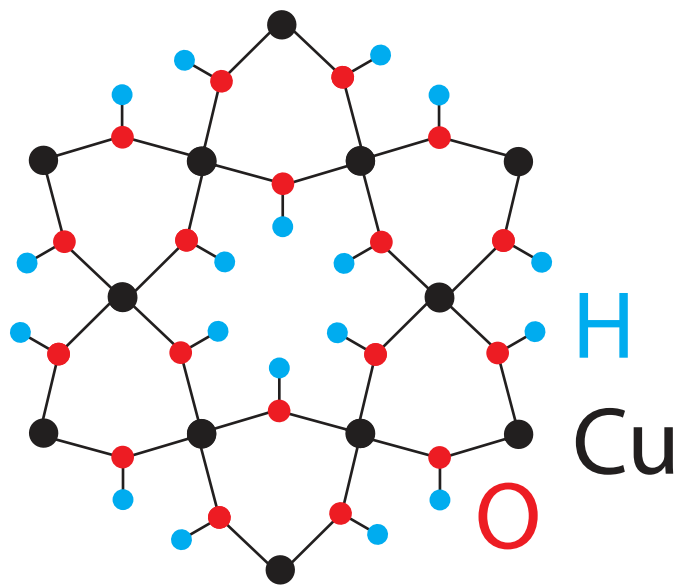
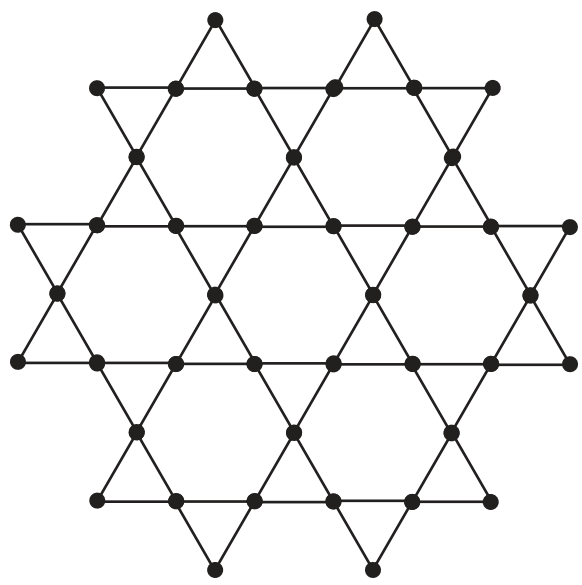
FIG. 1: Left : A Kagomé lattice. Right :  $\text{Cu}^{2+}$  Kagomé layer in  $\text{ZnCu}_3(\text{OH})_6\text{Cl}_2$ .  $\text{Cl}^-$  site is above or below the middle of the  $\text{Cu}^{2+}$  triangles.

FIG. 2: Typical  $^{35}\text{Cl}$  NMR lineshapes in 8.4 Tesla of the  $I_z = +\frac{1}{2}$  to  $-\frac{1}{2}$  central transition in a partially uniaxially aligned ceramic sample. The sharp peak near 35.02 MHz marked as “ $B//c$ ” originates from the ceramic particles whose  $c$ -axis is aligned along the external magnetic field. Vertical gray line is a guide for eyes to show the shift of the  $c$ -axis peak and edge. Vertical arrows specify the frequency corresponding to  $^{35}K_{1/2}$ .

FIG. 3:  $^{35}\text{Cl}$  NMR Knight shift (left scale).  $^{35}K_{peak}$  (black circles).  $^{35}K_{edge}$  (blue circles).  $^{35}K_{1/2}$  (red triangles). The solid line is a fit to a Curie-Weiss behavior,  $^{35}K_{peak} = (22 \pm 7)/(T - \theta_{CW}) + ^{35}K_{chem}$ , where  $\theta_{CW} = -240 \pm 80\text{K}$ . The constant background  $^{35}K_{chem} = 0.018\%$  is shown by a dashed line.  $\chi_{bulk}$  measured by SQUID (green cross) is also overlayed (right scale).

FIG. 4: Temperature dependence of  $^{35}\text{Cl}$  and  $^{63}\text{Cu}$  NMR spin-lattice relaxation rate  $1/T_1$ . (Inset)  $1/T_1T$ . Red curve is a fit to a Curie-Weiss law with a constant background,  $^{63}(1/T_1T) = 95 + 1027/(T - \theta) \text{ sec}^{-1}\text{K}^{-1}$  with  $\theta = -1.2 \pm 1.0 \text{ K}$ . Blue curve is a fit to a power law,  $^{63}(1/T_1T) = T^{\alpha-1}$  with  $\alpha = 0.47$ .

FIG. 5: Cu NQR (in zero external magnetic field) and NMR (7.9 Tesla) lineshapes observed at 4.2 K for unaligned ceramic sample.  $^{63}(1/T_1)$  was measured by NMR at the edge of  $^{63}\text{Cu}$  central peak as marked by an arrow.



H  
Cu  
O

